CrossMark

# Prediction of dominant intraseasonal modes in the East Asian-western North Pacific summer monsoon

Hyoeun Oh[1] · Kyung-Ja Ha[1]

© Springer-Verlag Berlin Heidelberg 2015

**Abstract** Intraseasonal monsoon prediction is the most imperative task, but there remains an enduring challenge in climate science. The present study aims to provide a physical understanding of the sources for prediction of dominant intraseasonal modes in the East Asian-western North Pacific summer monsoon (EA-WNPSM): pre-Meiyu&Baiu, Changma&Meiyu, WNPSM, and monsoon gyre modes classified by the self-organizing map analysis. Here, we use stepwise regression to determine the predictors for the four modes in the EA-WNPSM. The selected predictors are based on the persistent and tendency signals of the sea surface temperature (SST)/2m air temperature and sea level pressure fields, which reflect the asymmetric response to the El Niño Southern Oscillation (ENSO) and the ocean and land surface anomalous conditions. For the pre-Meiyu&Baiu mode, the SST cooling tendency over the western North Pacific (WNP), which persists into summer, is the distinguishing contributor that results in strong baroclinic instability. A major precursor for the Changma&Meiyu mode is related to the WNP subtropical high, induced by the persistent SST difference between the Indian Ocean and the western Pacific. The WNPSM mode is mostly affected by the Pacific-Japan pattern, and monsoon gyre mode is primarily associated with a persistent SST cooling over the tropical Indian Ocean by the preceding ENSO signal. This study carries important implications for prediction by establishing valuable precursors of the four modes including nonlinear characteristics.

# 1 Introduction

The intraseasonal variability (ISV) of the East Asian-western North Pacific summer monsoon (EA-WNPSM), causing floods and droughts, links to the sequential passages of frontal systems, advance/retreat of the western North Pacific subtropical high (WNPSH), and tropical cyclone (TC) during June–July–August (JJA; Chen et al. 2004). On the intraseasonal time scale, the East Asian summer monsoon (EASM) is categorized as the Changma (in Korea), Meiyu (in China), and Baiu (in Japan) with remarkable differences in their characteristics and rainy periods (Chang et al. 1998; Kang et al. 1999; LinHo and Wang 2002; Qian et al. 2002; Ha et al. 2005; Ha and Lee 2007). Wang and Xu (1997) have shown statically significant climatological intraseasonal oscillations (CISOs), which are considered as phase-locking of ISOs. However, the summer monsoon ISO is not always phase-locked (Wang and Rui 1990). Due to its irregularity and complexity, understanding nonlinear characteristics and establishing physical sources of prediction over the EA-WNPSM region are crucial problems, with the aim of reducing social and economic losses (Yoo et al. 2010a).

The skillful prediction of the EA-WNPSM is an imperative, but difficult task because of the prominent seasonal migration of the monsoon rainband from May to August (Tao and Chen 1987) and various processes that govern the monsoon circulation (Wang et al. 2000, 2008b; Wu et al. 2009; Zhou and Zou 2010; among others). The previous

✉ Kyung-Ja Ha
  kjha@pusan.ac.kr

[1] Division of Earth Environmental System, Pusan National University, 609-735 Busan, Korea

studies have mentioned that the mechanisms to influence EA-WNPSM variability are recognized as the El Niño-Southern Oscillation (ENSO), Indian Ocean (IO), western Pacific (WP) thermal statuses (Chang et al. 1998; Wang et al. 2000; Lau et al. 2000; Lau and Wu 2001; Yun et al. 2008, 2009; Xie et al. 2009), the North Atlantic Oscillation (Wu et al. 2009), Tibetan Plateau warming via two distinct Rossby wave trains (Wu et al. 2007; Wang et al. 2008a), spring Eurasian snow cover (Yang and Xu 1994; Liu and Yanai 2002; Yim et al. 2010), and spring Arctic Oscillation (Gong and Ho 2003; Gong et al. 2011) as well. Wang et al. (2013) showed the current coupled climate models have limited skills in the seasonal prediction of the EASM precipitation in general, even though their skills have been steadily improved. They also compared prediction skills of the dynamical models' multi-model ensemble (MME) and physical–empirical (P–E) model and concluded that the MME generated better results for the WNPSM rainfall, while the P–E model was better for predicting the EASM land rainfall (Wang et al. 2015).

Chu et al. (2012) identified four major intraseasonal modes in the EA-WNPSM, classified by a self-organizing map (SOM) analysis. They also demonstrated that the four modes can be regarded as components of the monsoon ISO, which is the phase locked to the seasonal cycle to a certain degree. Oh and Ha (2015) (hereinafter referred to as OH15) discussed the distinct instability with dynamic-thermodynamic characteristics by underlying their regional features. Following previous studies (Chu et al. 2012; OH15), our objective is to provide primary sources to predict the four intraseasonal modes in the EA-WNPSM using the P–E model. It carries important implications for prediction to build on meaningful and proper precursors of the four modes including nonlinear characteristics. For a broader scope, we changed the names of the four modes from previous studies to pre-Meiyu&Baiu (SOM1), Changma&Meiyu (SOM2), WNPSM (SOM3), and monsoon gyre (SOM4) modes, respectively.

To address the physical processes that drive interannual changes with the ultimate goal of assessing the prediction of the EA-WNPSM, we attempt to use persistent and tendency precursors. The persistence signals for January–April (JFMA)/February–May (FMAM) and the tendency indicates April–May minus February–March (AM minus FM)/April minus March. The tendency signals indicate the direction of the anomaly development. To objectively and physically select consequential predictors, we focus on

the SST/2m air temperature over land (T2m) and sea level pressure (SLP) field, which reflect the ocean and land surface anomalous conditions (Wang et al. 2015; Yim et al. 2015).

The next section describes observational datasets and methods used in this study. Section 3 describes the primary sources to predict the four modes. Section 4 addresses the prediction of the principal components, and the last contains our major results and discussion.

## 2 Data and methods

### 2.1 Observational datasets and methods

The present study used daily geopotential height at 850 hPa obtained from the National Centers for Environmental Prediction-Department of Energy (NCEP-DOE) Reanalysis 2 (NCEP2; Kanamitsu et al. 2002) and daily large-scale circulation fields (low-level winds, geopotential height, upper-level zonal wind) from NCEP-National Center for Atmospheric Research (NCAR) (NCEP1; Kalnay et al. 1996) during the period of 1979–2012. The daily large-scale circulation fields are used as input datasets of the SOM. The SST data for the period 1979–2012 was obtained from the Hadley Centre Sea Ice and Sea Surface Temperature dataset (HadISST) made available by the British Atmospheric Data Centre (BADC) (Rayner et al. 2003). Daily precipitation data was collected from the Tropical Rainfall Measuring Mission (TRMM) precipitation feature database 3B42 (multi-satellite) for 1998–2012. Since the daily TRMM 3B42 began in January 1998, no earlier data was available.

Here we use stepwise regression to establish prediction equations. The stepwise procedure has a virtue to choose important predictors from the larger potential predictors on the basis of a 95 % statistical significance level, so that the selected predictors are simple, yet have a good predictive ability. To directly compare the relative contributions of each predictor, all independent variables are normalized and highly significant according to an F-test procedure.

### 2.2 Extraction of four SOM modes

The SOM is a clustering algorithm and type of an unsupervised learning to classify the training data without any external information, which is related to feedforward networks (Kohonen 1990). This approach was first

proposed by Chattopadhyay et al. (2008) for the Indian monsoon and has been applied to distinguish the dominant intraseasonal modes in the EASM by Chu et al. (2012) and OH15. Following previous studies (Chu et al. 2012; OH15), we adjust their SOM analysis, of which input data is used as six daily dynamical monsoon indices representing the western North Pacific subtropical high (WNPSH), upper-level vorticity, vertical wind shear, and low-level southeasterlies (Wang et al. 1998; Lau et al. 2000; Wang et al. 2001; Ha et al. 2005). A detailed description of the input data is presented in Chu et al. (2012). The method classifies the data in a specified number of SOM patterns on the basis of the least

Euclidean distance between the SOM patterns and observations (Kohonen 1990). Before selecting the four dominant SOM patterns, 3 by 3 maps were determined by Chu and Ha (2011). The 3 by 3 SOM patterns were chosen based on two criteria: (1) the number of clustered days for each SOM pattern should be large enough to capture the observed daily fields and (2) the number of SOM patterns should be small enough to describe the distinct intraseasonal patterns. They determined the four modes on the basis of their spatial and temporal information. The four SOM spatial patterns of the precipitation field corresponding to the day clustered at the respective mode show the major variability in the EA-WNPSM
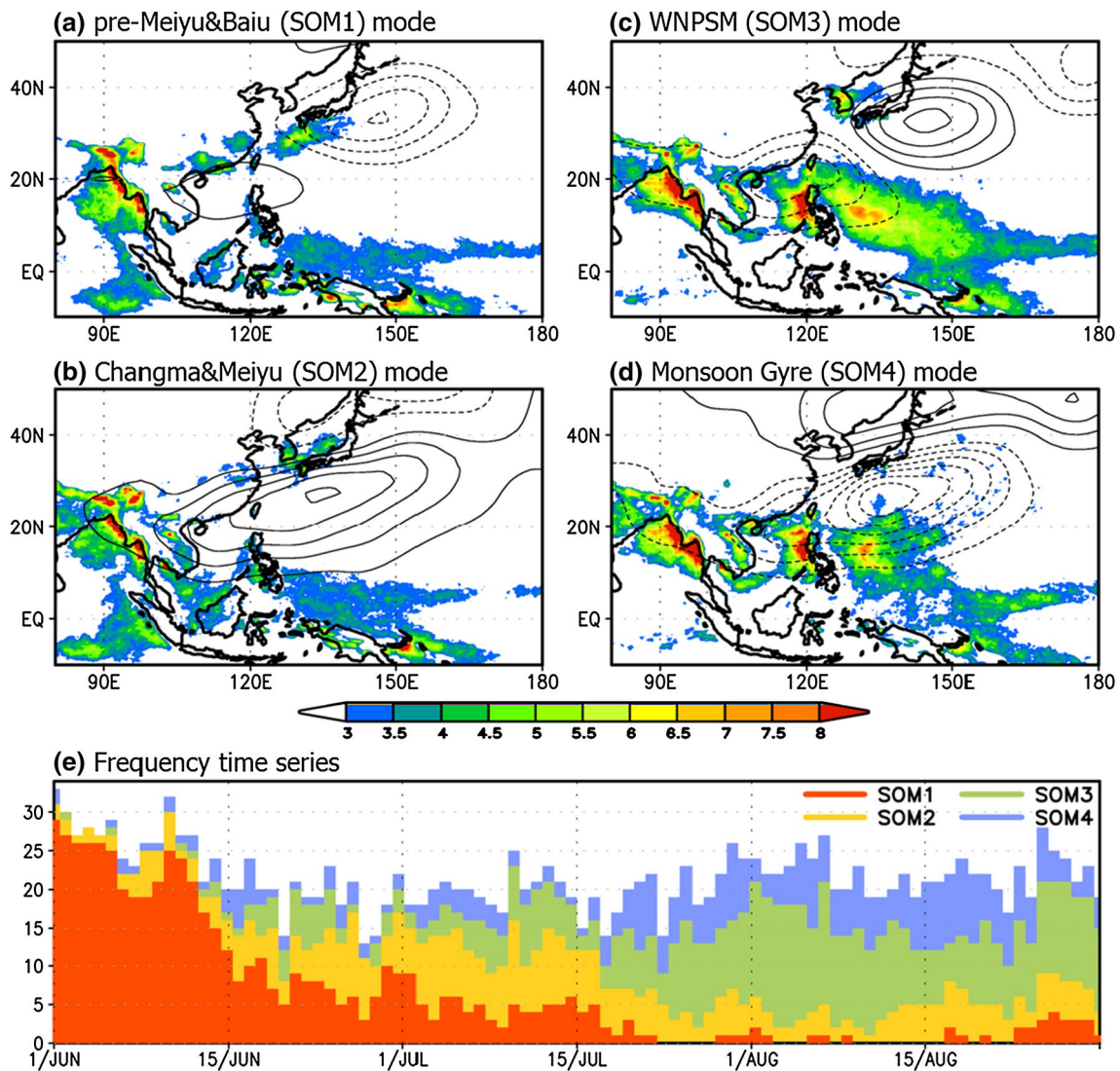


**Fig. 1 a–d** Spatial distribution of precipitation from 1998 to 2012 (*shading*) and 850 hPa geopotential heights from 1979 to 2012 (*contour*) associated with the four dominant self-organizing map (SOM) patterns obtained by compositing the daily data and **e** corresponding clustered days for each mode. The *lower column* shows the frequency time series as the number of days for each June–July–August (JJA) period

**Fig. 2** The annual number of days clustered at the four modes during 1979–2012
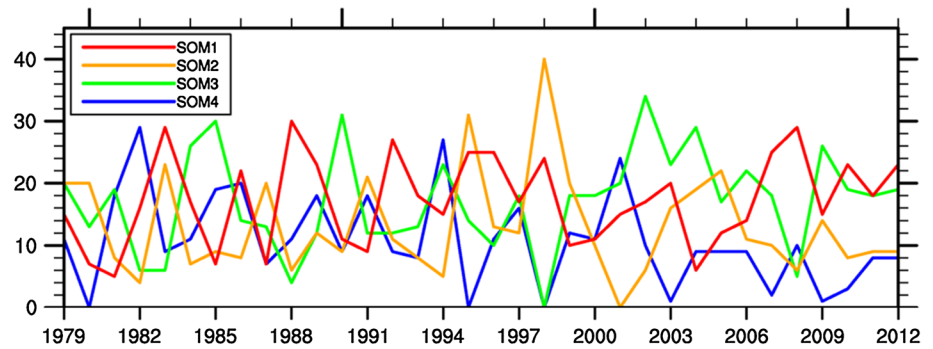


(Fig. 1a–e). The four modes account for more than 60 % of the total frequency (Fig. 1e). The modes can divide themselves roughly into two classes, which are associated with more frequent occurrences: early summer (SOM1 and SOM2) and late summer (SOM3 and SOM4) modes. A detailed description of the SOM can be found in OH15. Note that there are slight changes of the name for the four modes.

## 3 Physical precursors for the dominant intraseasonal modes

To improve the quality of prediction over the EA-WNPSM region, four dominant intraseasonal modes are identified by the SOM analysis. Because of the nonlinear variability of monsoon rainfall, it is difficult but necessary to predict the intraseasonal precipitation of the EA-WNPSM. In order to reduce social and economic losses, our objective in this study is to develop a physical understanding of the sources for prediction over the EA-WNPSM region, using interannual variability (IAV) of the SOM patterns. The IAV is represented as annual occurrences in a particular mode, which is defined by counting the number of days in a year (Fig. 2; OH15). The prediction of the IAV helps to understand how many times the modes appear at the specific time period in a year.

To objectively and physically select consequential predictors, we focus on the SST/T2m and SLP, which reflect the ocean and land surface anomalous conditions and use the P–E model with persistency and tendency precursors. Stepwise regression analysis is used to set the prediction equation on the basis of a 95 % statistical significance level and to verify the relative independence of the selected predictors.
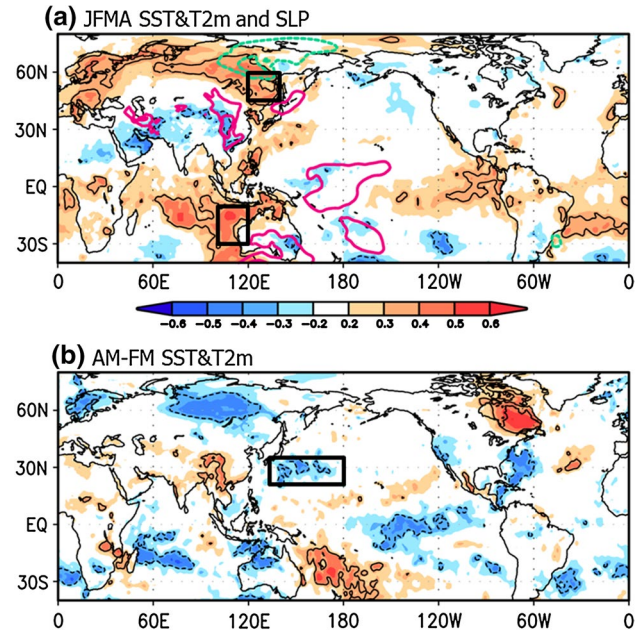


**Fig. 3** Predictors selection based on the correlation maps of the **a** anomalous January–February–March–April (JFMA) mean SST/T2 m (*shading*) and SLP (*contour*) and **b** anomalous April–May (AM) minus February–March (FM) SST/T2 m regarding the interannual variability (IAV) indicated by the annual number of days clustered in the pre-Meiyu&Baiu (SOM1) mode. The *pink solid* (*green dashed*) contour indicates *positive* (*negative*) correlation coefficient between SLP and SOM1 time series starting from 0.339, which is the value exceeding 95 % confidence level, with an interval of 0.1. The *black contour* indicates the areas exceeding 95 % confidence level for SST/T2 m. The *black bold boxes* are the region of defining predictors

### 3.1 Pre-Meiyu&Baiu (SOM1) mode

The pre-Meiyu&Baiu mode is characterized by a zonally elongated jet stream which represents an anomalous cyclonic vorticity over the Asian jet exit region. In
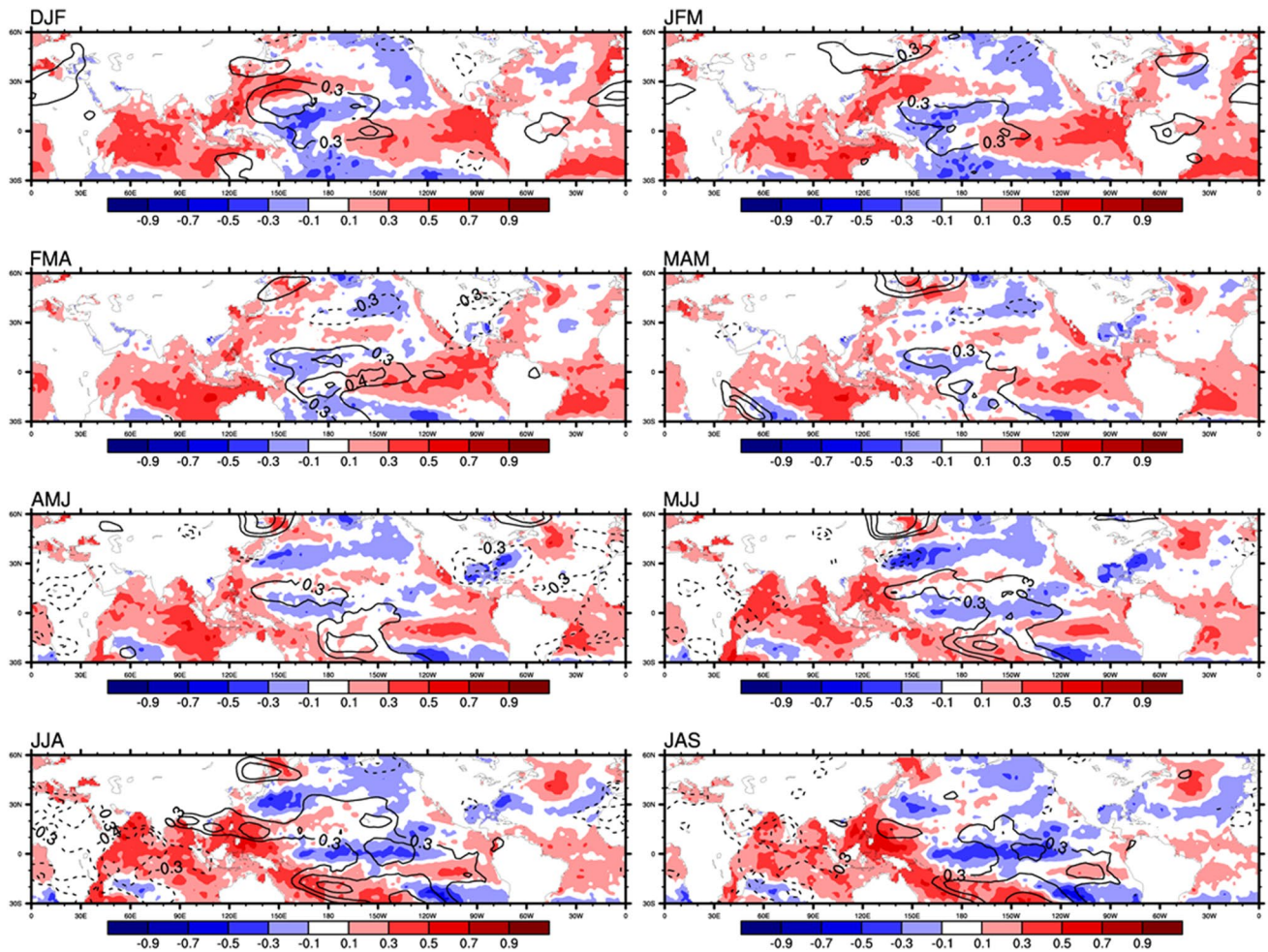
**Fig. 4** Seasonal sequence of the correlation coefficients with SST (*shading*) and geopotential height at 850 hPa (*contour*) for pre-Meiyu&Baiu (SOM1) mode. The contour interval is 0.1

addition, the mode is linked to baroclinic instability, resulting from the strong meridional temperature gradient through a thermal wind relationship (Sampe and Xie 2010; OH15). A first predictor is land warming over northeast Asia [120°–140°E, 45°–60°N] that persists from JF to MA (Fig. 3a). One possible explanation for the persistent warming over the northeast Asia is attributed to a persistent anticyclone anomaly from preceding winter to concurrent summer (Fig. 4). The warming over the northeast Asia brings about propagating an anomalous cyclonic circulation to the southern part of the anomalous anticyclone along the wave propagation. To test the warming influence on this mode, we mimicked a virtual forcing with a linear baroclinic model

(LBM) and confirmed that the anomalous low over southern Japan was preceded by the warming over the northeast Asia (Figure not shown). It has been pointed out by Yim et al. (2010) that the warming over the northeast Asia foreshadowed a development of the anomalous cyclonic circulation in early summer, with a rainfall enhancement over East Asia. The anomalous cyclonic circulation cools Kuroshio SST through reducing downward solar radiation reaching the surface. The cooling tendency lasts until JJA, which reflects a deepening of the cyclone. Thus, a second predictor is defined as the Kuroshio cooling signal on the AM minus FM SST tendency field [130°–180°E, 20°–35°N] (Fig. 3b). The cooling tendency there will enhance the SST meridional gradient that reflects strong

baroclinic instability. A strengthened and southward-shifted wind shear, related to the baroclinic instability, is found from the following spring to summer period (Figure not shown), and the southward jet stream tends to increase droughts in northern China and floods in the southern China (Yu et al. 2004).

The anomalous anticyclonic circulation over the WNP region exists, together with the enhanced summertime north Pacific subtropical high (NPSH) in this mode. Yun et al. (2015) showed that the in-phase relationship between the WNPSH and NPSH is associated with the quasi-biennial-type ENSO, showing a fast phase transition from warm to cold phases. Figure 4 shows an abrupt termination of the El Niño phase that evolves into the La Niño phase from preceding December–January–February (DJF) to JJA. Thus, the eastern Pacific SST anomaly itself could not directly influence this mode. Instead, a persistent Eastern IO SST warming, affected by the preceding wintertime ENSO, is a third predictor (Fig. 3a). The persistent warming signal over the eastern IO [100°–120°E, 30°–10°S] leads to warming over the maritime continent, hence, it helps to maintain the subtropical high in Fig. 4 (Wang et al. 2013). The mode features that the anomalous anticyclonic circulation causes the anomalous cyclonic circulation over the southern Japan through the Rossby wave train, but intensity of the anticyclone is weaker than the SOM2. The anomalous cyclonic circulation produces the enhanced rainfall in the mode as a result.

### 3.2 Changma&Meiyu (SOM2) mode

The Changma&Meiyu mode is associated with advection of moist and warm air by strong southwesterly winds along the northwestern flank of the WNPSH (Fig. 1b). The southwesterly winds along the WNPSH cause convective instability, triggered by warm, moist air at the low-level and cold, dry air at the upper-level from the north (OH15). The Changma&Meiyu mode is strongly related to the preceding ENSO through the WNPSH that is an evidence of a strong tropical–subtropical connection in Fig. 6 (Wang et al. 2000). Because of the WNPSH, a northward-shifted and localized rainband with intense precipitation over the Korean Peninsula and suppressed convection over the WNP are represented (Fig. 1b). Then, how can the WNPSH sustain itself until summertime? The interaction between the northern IO warming and WNPSH
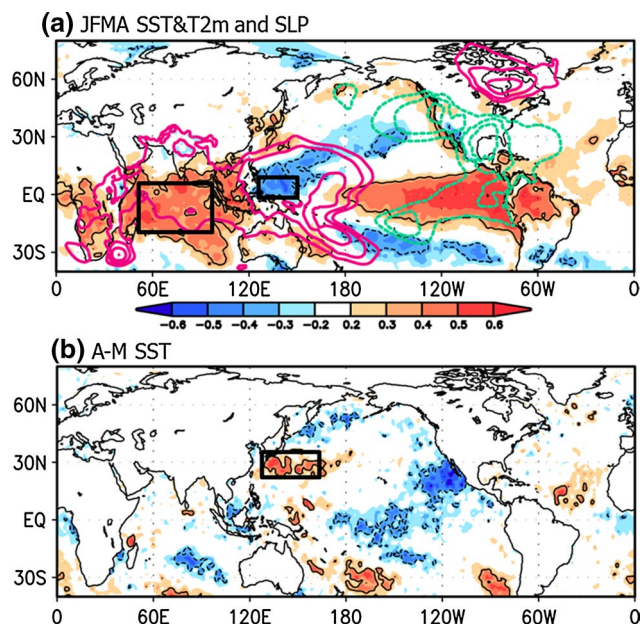


**Fig. 5** Predictors selection based on the correlation maps of the **a** anomalous January–February–March–April (JFMA) mean SST/T2 m (*shading*) and SLP (*contour*) and **b** anomalous SST difference between April and March regarding the interannual variability (IAV) indicated by the annual number of days clustered in the Changma&Meiyu (SOM2) mode The *pink solid* (*green dashed*) contour indicates *positive* (*negative*) correlation coefficient between SLP and SOM2 time series starting from 0.339, which is the value exceeding 95 % confidence level, with an interval of 0.1. The *black contour* indicates the areas exceeding 95 % confidence level for SST/T2 m. The *black bold boxes* are the region of defining predictors

can contribute to the maintenance of the subtropical high. The northern IO warming result from the southwestward extension of the WNPSH and it can enhance the anticyclone by generating an atmospheric Kevin wave response (Wang et al. 2013). In addition, the resultant WP cooling to the southeast of the WNPSH, due to wind-evaporation-SST feedback, reduces precipitation heating and it can generate a descending Rossby wave that strengthens the WNPSH (Wang et al. 2000, 2013). Both a warming over the IO and weak cooling over the WNP forced by the preceding ENSO through the Walker circulation generate a Rossby wave train. As a result, the anomalous anticyclone over the WNP region plays an important role in predicting this mode (Yun et al. 2008). Thus, a first predictor is the persistent SST difference between the IO [50°–100°E, 20°S–5°N] and WP [125°–150°E, 0°–10°N] (Fig. 5a).
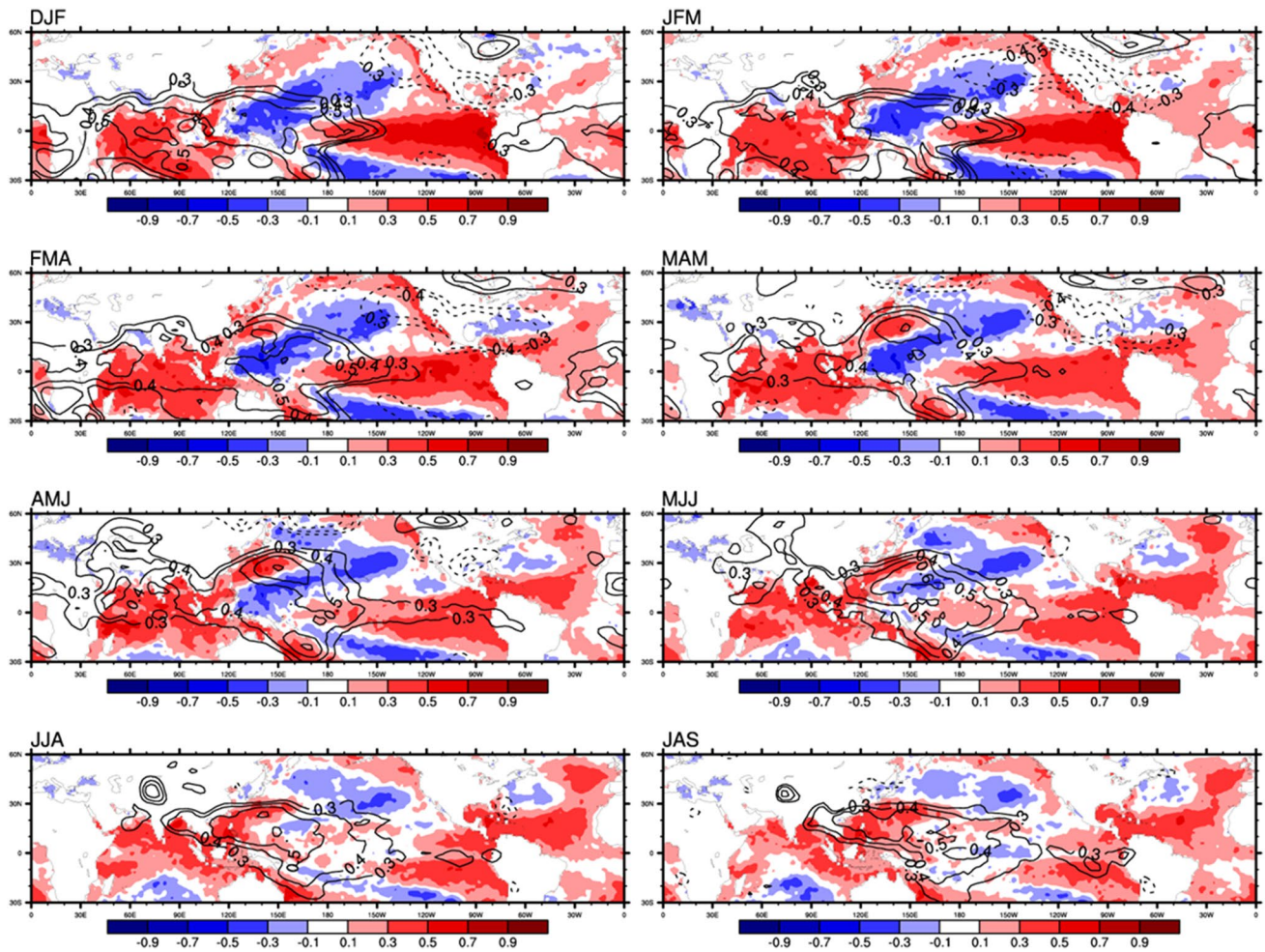
**Fig. 6** Same as Fig. 4 but for the Changma&Meiyu (SOM2) mode

Furthermore, localized rainfall over the Korean Peninsula prevails in this mode, so that we select the warming tendency between April and March over the Kuroshio region [130°–160°E, 25°–35°N] as a short temporal scale (Fig. 5b). The abrupt Kuroshio warming tendency may be concomitant with the strength of the anticyclonic circulation, indicating a link with the wind-driven circulation by air-sea interaction (Fig. 6).

### 3.3 WNPSM (SOM3) mode

In the WNPSM mode, a strong cyclonic circulation anomaly over the WNP, with intense precipitation, and an anticyclonic circulation anomaly over southern Japan are represented (OH15). The anomalous cyclonic circulation induces convective activity over the WNP, while the anticyclonic circulation over southern Japan leads to southeasterly wind that brings warm, moist air to the Korean Peninsula. The circulation patterns are considered as the Pacific-Japan (PJ) teleconnection pattern (Nitta 1987). A first predictor is associated with a persistent warming over the WP region [140°–170°E, 10°S–10°N] (Fig. 7a), which causes an increased deep convection through enhanced evaporation. The PJ pattern has relevance to the propagation of the convection over the WP region extending from tropics into the mid-latitudes in JJA (Fig. 8). Due to the anomalous
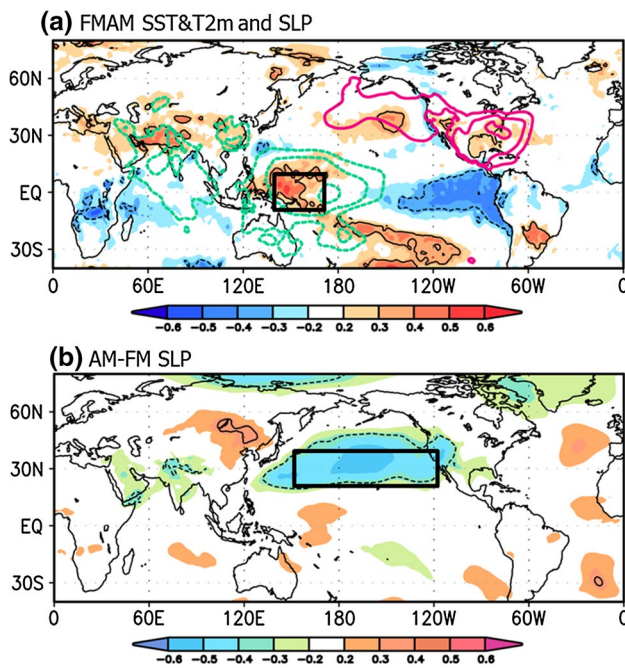
**Fig. 7** Predictors selection based on the correlation maps of the **a** anomalous February–March–April–May (FMAM) mean SST/T2 m (*shading*) and SLP (*contour*) and **b** anomalous April–May (AM) minus February–March (FM) SLP regarding the interannual variability (IAV) indicated by the annual number of days clustered in the WNPSM (SOM3) mode. The *pink solid* (*green dashed*) contour indicates *positive* (*negative*) correlation coefficient between SLP and SOM3 time series starting from 0.339, which is the value exceeding 95 % confidence level, with an interval of 0.1. The *black contour* indicates the areas exceeding 95 % confidence level for SST/T2 m. The *black bold boxes* are the region of defining predictors

anticyclone over the southeast of Japan induced by PJ pattern, the Korean Peninsula is influenced by an abundant moist and warm air (Fig. 1c). In addition, the mode is strongly correlated with typhoon activity at a 99 % confidence level with a correlation coefficient (CC) (0.49**). It has been agreed that the PJ pattern influences the TC activity (Choi et al. 2010). A second predictor is SLP tendency over the north Pacific (NP) [150°–240°E, 20°–40°N] (Fig. 7b). A meridional expansion of the anomalous cyclonic circulation over the WP leads to the simultaneous northward retreat of the anticyclonic circulation over the NP region (Fig. 8) (Li and Wang 2005). As the evidence of these relationships, we found that the two selected precursors are correlated with each other at the 90 % confidence level with a CC of −0.3, and those results suggest the robustness of the PJ teleconnection pattern.

## 3.4 Monsoon gyre (SOM4) mode

The cold, dry easterly flow over East Asia produced by the anomalous cyclonic circulation over the WNP results in suppressed precipitation by terminating moisture transport in the monsoon gyre mode (Fig. 1d; OH 15). This mode is related to significant persistent SST signals over the IO and Atlantic. Even though this mode can be explained by both the IO and Atlantic cooling, we focus on the IO cooling as a predictor, ruling out the Atlantic cooling effect. This is because the two regions are not independent, i.e. a significant relationship between the IO and Atlantic cooling has been identified. Figure 9 shows the correlation map of the SST/T2m and SLP. As a predictor, we select the IO cooling [50°–120°E, 25°S–10°N], which is triggered by the decaying phase of La Niña. The signal plays an essential role in weakening the WNPSH, with opposite to the Changma&Meiyu mode. It has been agreed that the IAV of the monsoon gyre mode shows a negative correlation with that of the Changma&Meiyu mode (CC of −0.53) (OH 15). Thus, the two modes have the similar predictors. The resultant IO cooling, followed by the termination of La Niña, is continuous with a northward propagation of Rossby waves by a deep convection over WP (Fig. 1d and Fig. 10; Lau and Peno 1992; Yoo et al. 2010b). The anomalous cyclonic circulation over the WP is highly correlated with the mode in conjunction with a weak EASM.

## 4 Prediction of the principal components

We have found the distinguishing predictors for the dominant modes in the EA-WNPSM and have attempted to predict the four modes through stepwise regression analysis. The interpretation establishes the physical consideration for prediction of the empirical patterns. The prediction equations and predictors definition are presented in detail in Table 1. For each prediction equation, the all independent variables fit a 95 % significance level based on an F-test. Figure 11 shows the temporal correlation skills for the prediction using the cross-validated method. To check the predictive capability of the P–E model, the cross-validation is performed by removing 3 years from each step (Michaelsen 1987). The cross-validated correlation skills between the IAV and the prediction for each mode show the significant correlations at a 95 % confidence level, with CCs of 0.63, 0.64, 0.54, and 0.54 in sequence. It demonstrates that the
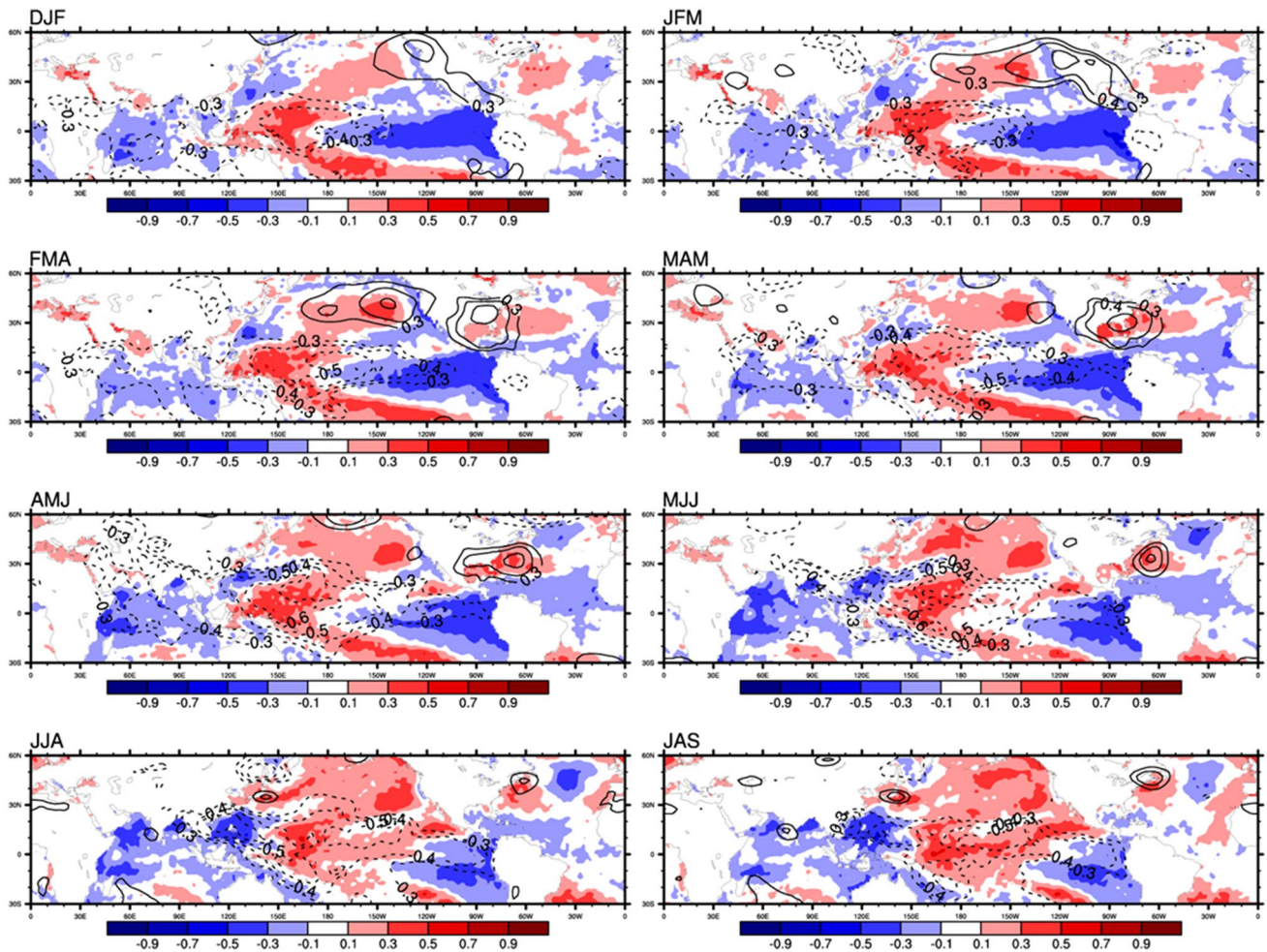
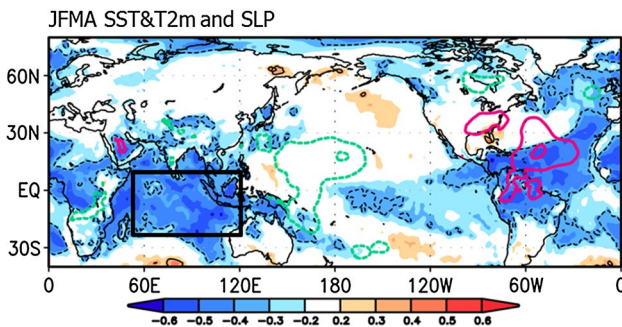**Fig. 8** Same as Fig. 4 but for the WNPSM (SOM3) mode



**Fig. 9** Predictors selection based on the correlation maps of the anomalous January–February–March–April (JFMA) mean SST/T2 m (*shading*) and SLP (*contour*) regarding the interannual variability (IAV) indicated by the annual number of days clustered in the monsoon gyre (SOM4) mode. The *pink solid* (*green dashed*) contour indicates *positive* (*negative*) correlation coefficient between SLP and SOM4 time series starting from 0.339, which is the value exceeding 95 % confidence level, with an interval of 0.1. The *black contour* indicates the areas exceeding 95 % confidence level for SST/T2 m. The *black bold box* is the region of defining predictor

four modes can be predicted with significant skills from 0.54 to 0.64.

The persistent warming over the northern East Asia and SST cooling tendency over the Kuroshio Current are distinctive precursors for the pre-Meiyu&Baiu (SOM1) mode. Both the precursors are linked to an anomalous cyclonic circulation at the mid-latitude. The Changma&Meiyu (SOM2) mode is sustained by the thermodynamic feedback between the WNPSH and underlying SST difference between IO and WP, which is mainly affected by the preceding ENSO (Yun et al. 2008). For the WNPSM (SOM3) mode, the persistent warming SST and deepened convection over the WP are key factors of prediction. This mode is evenly supported by the PJ teleconnection pattern, propagating the Rossby wave and extending it to the mid-latitudes. The monsoon gyre (SOM4) mode is associated with the resultant IO cooling followed by the preceding La Niña, which makes the WNPSH get weakened.
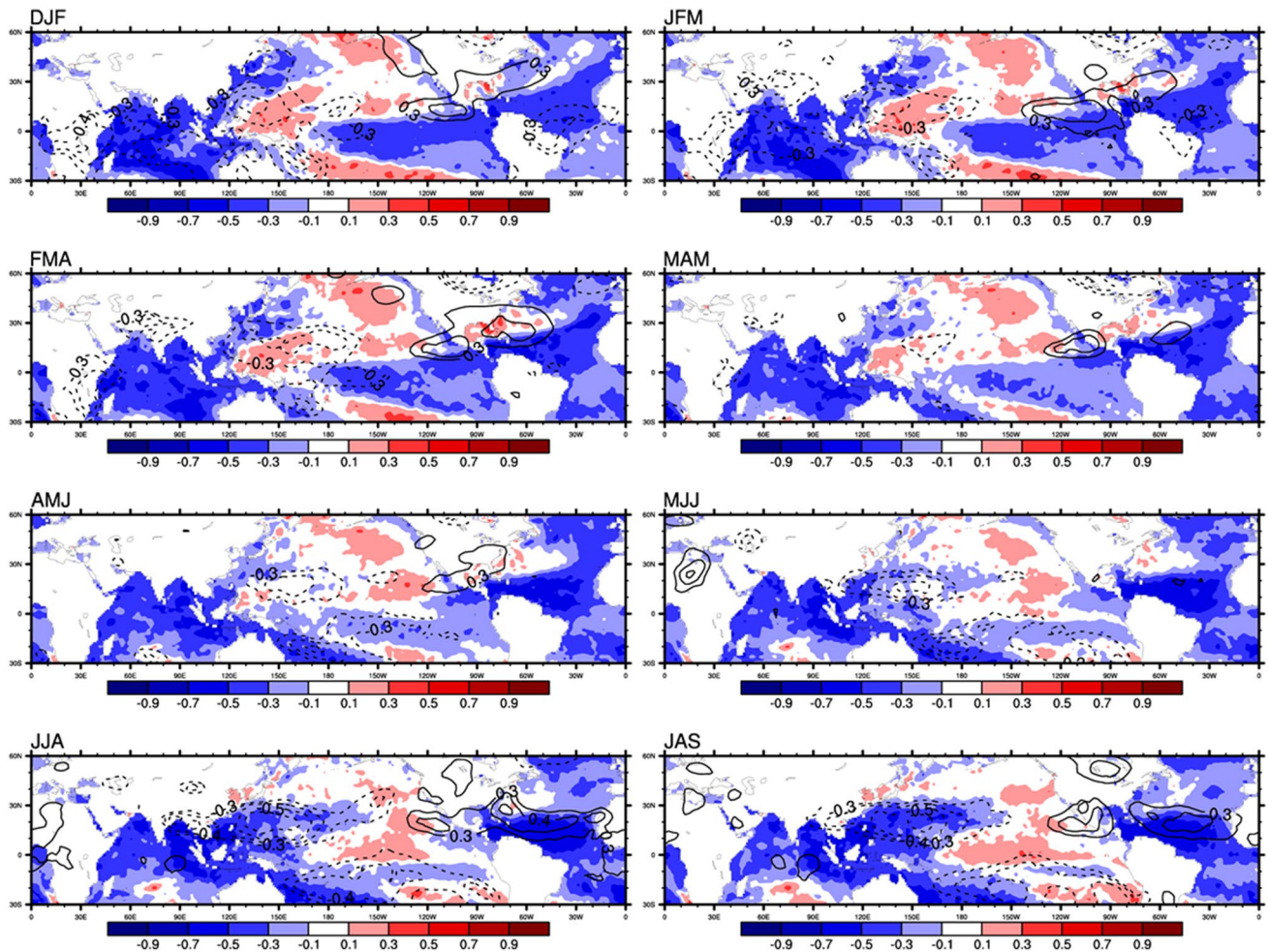
**Fig. 10** Same as Fig. 4 but for the monsoon gyre (SOM4) mode

**Table 1** Definition of the selected each predictor for prediction and corresponding simulation equations for the four modes

| Mode | Name | Definition | Prediction equation |
|------|------|-----------|---------------------|
| Pre-Meiyu&Baiu | JFMA NEA T2 m | [120°–140°E, 45°–60°N] | SOM1 = 0.411*[1. JFMA NEA T2 m] |
| | AM-FM Kuroshio SST | [130°–180°E, 20°–35°N] | −0.356*[2. AM-FM Kuroshio SST] |
| | JFMA EIO SST | [100°–120°E, 30°–10°S] | + 0.449*[3. JFMA EIO SST] |
| Changma&Meiyu | JFMA IO-WP SST | [50°–100°E, 20°S–5°N] −[125°–150°E, 0°–10°N] | SOM2 = 0.514*[1. JFMA IO-WP SST] + 0.392*[2. A-M Kuroshio SST] |
| | A-M Kuroshio SST | [130°–160°E, 25°–35°N] | |
| WNPSM | FMAM WP SST | [140°–170°E, 10°S–10°N] | SOM3 = 0.292*[1. FMAM WP SST] |
| | AM-FM NP SLP | [150°–240°E, 20°–40°N] | −0.491*[2. AM-FM NP SLP] |
| Monsoon gyre | JFMA IO SST | [50°–120°E, 25°S–10°N] | SOM4 = − 0.591*[1. JFMA IO SST] |

Prediction of dominant intraseasonal modes in the East Asian-western North Pacific summer...
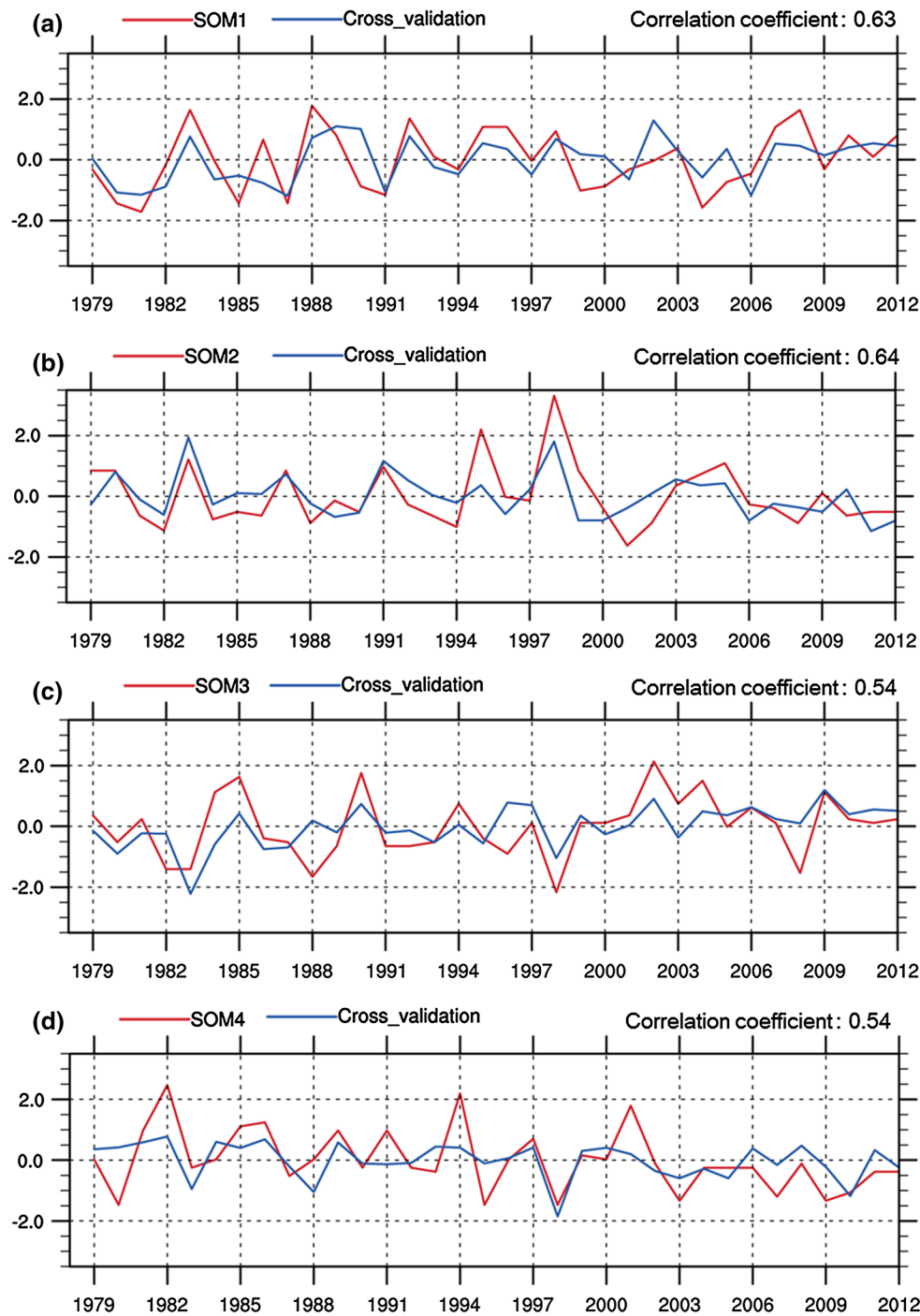
2035



**Fig. 11 a–d** The predicted and cross-validated predictions for the four SOM modes during 1979–2012. The cross-validation was done by removing three years around the predicted year

## 5 Summary and discussion

In the present study, we have investigated the sources of predictability for the four dominant modes in the EA-WNPSM and have established the P–E model by developing a physical understanding of the sources. To objectively and physically select the consequential predictors, we focused on the SST/T2m and SLP, based on the asymmetric response to the ENSO, the ocean and land surface anomalous conditions. The physically meaningful and statistically robust predictors were selected based on the persistency (i.e. JFMA and FMAM) and tendency (i.e. AM minus FM

and April minus March). To establish the prediction equations, we used the stepwise regression. The regression has a virtue to identify important predictors from the larger potential predictors on the basis of a 95 % statistical significance level. The selected important predictors on the basis of the stepwise regression proved the statistical significance and relative independence. To check the prediction skills of the empirical model, we adjusted the cross-validation method to remove 3 years from each step (Michaelsen 1987). The cross-validated correlation skills between the predictions and IAV are significant. The cross-validated prediction results demonstrated that the four modes could be predicted with significant skills ranging from 0.54 to 0.64.

The four modes together explained more than 60 % of the total variance. For the pre-Meiyu&Baiu mode, the SST cooling tendency over the Kuroshio Current was the most distinct predictor and it could modulate the strong vertical wind shear, linked to the baroclinic instability. Two other predictors were relevant to induce the associated circulation field. There was a strong connection between the Changma&Meiyu mode and WNPSH that plays an important role in predicting the mode. The IO warming and WNP cooling through the Walker circulation generated a Rossby wave train. Additionally, the abrupt Kuroshio warming tendency as a second predictor, associated with localized rainfall over the Korean Peninsula, was relevant to the wind-driven circulation by air-sea interaction. Precursors for the WNPSM and monsoon gyre modes in late summer were more difficult to find their precursors. A first predictor of the WNPSM mode had relevance to the persistent warming over the WP region. The warming induced a significant PJ teleconnection pattern. A second predictor was the decrease of pressure over the north Pacific, induced by the northward extension of the anomalous cyclone over the WP. The two predictors detected the associated circulation patterns in the WNPSM mode. The monsoon gyre mode was mostly linked to the persistent SST cooling over the IO and correlated with a weakened WNPSH. We demonstrated that the four intraseasonal modes, which involved the nonlinear rectification of the mean state by the asymmetric response to ENSO, could be predicted reasonably well by the statistical method. This study has important implications for prediction by establishing the physical precursors of the four dominant modes over the EA-WNPSM region.

We also found that the four modes have distinctive spatial structures and temporal variabilities by the preceding ENSO. Regarding the distinct response to ENSO for the four modes, impacts on the regional climate are not directly linked. Thus, ENSO indirectly affects the intraseasonal phases of the EA-WNPSM via a tropical atmospheric bridge, IO SST, Atlantic SST, and among others. The Indian and Atlantic Ocean affected by the preceding ENSO

have more influence on the Changma&Meiyu and monsoon gyre modes than the pre-Meiyu&Baiu and WNPSM modes. Their detailed mechanisms will be explored in the future.

# References

Chang CP, Hou SC, Kuo HC, Chen GTJ (1998) The development of an intense East Asian summer monsoon disturbance with strong vertical coupling. Mon Weather Rev 126:2692–2712

Chattopadhyay R, Sahai AK, Goswami BN (2008) Objective Identification of nonlinear convectively coupled phases of monsoon intraseasonal oscillation: implications for prediction. J Atmos Sci 65:1549–1569

Chen TC, Wang SY, Yen MC, Gallus Jr. WA (2004) Role of the monsoon gyre in the interannual variation of tropical cyclone formation over the western north pacific. Wea Forecast 19:776–785

Choi KS, Wu CC, Cha EJ (2010) Change of tropical cyclone activity by Pacific-Japan teleconnection pattern in the western North Pacific. J Geophys Res 115:D19114. doi:10.1029/2010JD013866

Chu JE, Ha KJ (2011) Classification of intraseasonal oscillation in precipitation using self-organizing map for the East Asian summer monsoon. Atmos Krn Meteorol Soc 21:221–228

Chu JE, Saji NH, Ha KJ (2012) Non-linear, intraseasonal phases of the East Asian summer monsoon: extraction and analysis using self-organizing maps. J Clim 25(20):6975–6988. doi:10.1175/JCLI-D-11-00512.1

Gong DY, Ho C-H (2003) Arctic oscillation signals in the East Asian summer monsoon. J Geophys Res 108(D2):4066. doi:10.1029/2002JD002193

Gong DY, Yang J, Kim SJ, Gao Y, Guo D, Zhou T, Hu M (2011) Spring Arctic Oscillation-East Asian summer monsoon connection through circulation changes over the western North Pacific. Clim Dyn 37:2199–2216

Ha KJ, Lee SS (2007) On the interannual variability of the Bonin high associated with the East Asian summer monsoon rain. Clim Dyn 28:67–83. doi:10.1007/s00382-006-0169-x

Ha KJ, Park SK, Kim KY (2005) On interannual characteristics of climate prediction center merged analysis precipitation over the Korean peninsula during the summer monsoon season. Int J Climatol 25:99–116. doi:10.1002/joc.1116

Kalnay E et al (1996) The NCEP/NCAR 40-year reanalysis project. Bull Am Meteorol Soc 77:437–471

Kanamitsu M, Ebisuzaki W, Woollen J, Yang SK, Hnilo JJ, Fiorino M, Potter GL (2002) NCEP-DOE AMIP-II reanalysis (R-2). Bull Am Meteorol Soc 83:1631–1643

Kang IS, Ho CH, Lim YK (1999) Principal modes of climatological seasonal and intraseasonal variations of the Asian summer monsoon. Mon Weather Rev 127:322–340

Kohonen T (1990) The self-organizing map. Proc IEEE 78:1464–1480

Lau KM, Peno L (1992) Dynamics of atmospheric teleconnection during northern summer. J Atmos Sci 5:140–158

Lau KM, Wu HT (2001) Principal modes of rainfall-SST variability of the Asian summer monsoon: a reassessment of the monsoon-ENSO relationship. J Clim 14:2880–2895

Lau KM, Kim KM, Yang S (2000) Dynamical and boundary forcing characteristics of regional components of the Asian summer monsoon. J Clim 13:2461–2482

Li T, Wang B (2005) A review on the western North Pacific monsoon: synoptic-to-interannual variabilities. Terr Atmos Ocean Sci 16:285–314

LinHo, Wang B (2002) The time-space structure of the Asian-Pacific summer monsoon: a fast annual cycle view. J Clim 15:2001–2019

Liu X, Yanai M (2002) Influence of Eurasian spring snow cover on Asian summer rainfall. Int J Climatol 22:1075–1089

Michaelsen J (1987) Cross-validation in statistical climate forecast model. J Clim Appl Meteorol 26:1589–1600

Nitta T (1987) Convective activities in the tropical western Pacific and their impact on the Northern Hemisphere summer circulation. J Meteorol Soc Jpn 65:373–390

Oh H, Ha KJ (2015) Thermodynamic characteristics and responses to ENSO of dominant intraseasonal modes in the East Asian summer monsoon. Clim Dyn 44(7):1751–1766. doi:10.1007/s00382-014-2268-4

Qian W, Kang HS, Lee DK (2002) Distribution of seasonal rainfall in the East Asian monsoon region. Theor Appl Climatol 73:151–168

Rayner NA, Parker DE, Horton EB, Folland CK, Alexander LV, Rowell DP, Kent EC, Kaplan A (2003) Global analyses of sea surface temperature, sea ice, and night marine air temperature since the late nineteenth century. J Geophys Res 108(D14):4407

Sampe T, Xie SP (2010) Large-scale dynamics of the Meiyu-Baiu rainband: environmental forcing by the westerly jet. J Clim 23:113–134

Tao S, Chen L (1987) A review of recent research on the East Asia summer monsoon in Chin. In: Chang C-P, Krishnamurti TN (eds) Monsoon meteorology. Clarendon Press, Oxford, pp 60–92

Wang Q, Ding Y, Jiang Y (1998) Relationship between Asian monsoon activities and the precipitation over China mainland. Q J Appl Meteorol 9:84–89

Wang B, Rui H (1990) Synoptic climatology of transient tropical intraseasonal convection anomalies:1975–1985. Meteor Atmos Phys 44:43–61

Wang B, Wu R, Fu X (2000) Pacific-East Asia teleconnection: How does ENSO affect East Asian climate? J Clim 13:1517–1536

Wang B, Wu R, Lau KM (2001) Interannual variability of the Asian summer monsoon: contrasts between the Indian and the western north Pacific-east Asian monsoons. J Clim 14:4073–4090

Wang B, Bao Q, Hoskins B, Wu G, Liu Y (2008a) Tibetan Plateau warming and precipitation change in East Asia. Geophys Res Lett 35:L14702

Wang B, Wu Z, Li J, Liu J, Chang CP, Ding Y, Wu GX (2008b) How to measure the strength of the East Asian summer monsoon? J Clim 21:4449–4463

Wang B, Xu X (1997) Northern Hemisphere summer monsoon singularities and climatological intraseasonal oscillation. J Clim 10:1071–1085

Wang B, Xiang B, Lee JY (2013) Subtropical high predictability establishes a promising way for monsoon and tropical storm predictions. PNAS 110:2718–2722

Wang B, Lee JY, Xiang B (2015) Asian summer monsoon rainfall predictability: a predictable mode analysis. Clim Dyn. doi:10.1007/s00382-014-2218-1

Wu G, Liu Y, Zhang Q, Duan A, Wang T, Wan R, Liu X, Li W, Wang Z, Liang X (2007) The influence of mechanical and thermal forcing by the Tibetan Plateau on Asian climate. J Hydrometeorol 8:770–789

Wu Z, Wang B, Li J, Jin FF (2009) An empirical seasonal prediction model of the east Asian summer monsoon using ENSO and NAO. J Geophys Res 144:D18120

Xie SP, Hu K, Hafner J, Tokinaga H, Du Y, Huang G, Sampe T (2009) Indian Ocean capacitor effect on Indo-Western Pacific climate during the summer following El Niño. J Clim 22:730–747

Yang S, Xu L (1994) Linkage between Eurasian winter snow cover and regional Chinese summer rainfall. Int J Climatol 14:739–750. doi:10.1002/joc.3370140704

Yim SY, Jhun JG, Lu R, Wang B (2010) Two distinct patterns of spring Eurasian snow cover anomaly and their impacts on the East Asian summer monsoon. J Geophys Res 115:D22113

Yim SY, Wang B, Xing W, Lu MM (2015) Prediction of Meiyu rainfall in Taiwan by multi-lead physical-empirical models. Clim Dyn. doi:10.1007/s00382-014-2340-0

Yoo JH, Robertson AW, Kang IS (2010a) Analysis of intraseasonal and interannual variability of the Asian summer monsoon using a hidden Markov model. J Clim 23:5498–5516

Yoo SH, John F, Yang S, Ho CH (2010b) On the relationship between Indian Ocean sea surface temperature and the transition from El Niño to La Niña. J Geophys Res 115:D15114

Yu R, Wang B, Zhou T (2004) Tropospheric cooling and summer monsoon weakening trend over East Asia. Geophys Res Lett 31:L22212

Yun KS, Seo KH, Ha KJ (2008) Relationship between ENSO and Northward Propagating Intraseasonal Oscillation in the East Asian Summer Monsoon System. J Geophys Res 113:D14120. doi:10.1029/2008JD009901

Yun KS, Ren B, Ha KJ, Chan JCL, Jhun JG (2009) The 30–60-day oscillation in the East Asian summer monsoon and its time-dependent association with the ENSO. Tellus 61A:565–578. doi:10.1111/j.1600-0870.2009.00410.x

Yun KS, Ha KJ, Yeh SW, Wang B, Xiang B (2015) Critical role of boreal summer North Pacific subtropical highsin ENSO transition. Clim Dyn 44:1979–1992

Zhou T, Zou LW (2010) Understanding the predictability of East Asian summer monsoon from the reproduction of land-sea thermal contrast change in AMIP-type simulation. J Clim 23(22):6009–6026